



Contents lists available at [ScienceDirect](http://www.sciencedirect.com)

CIRP Annals Manufacturing Technology

Journal homepage: www.elsevier.com/locate/cirp



Investigations on turning Ti-6Al-4V titanium alloy using super-finished tool edge geometry generated by micro-machining process (MMP)

Anil K. Srivastava^a (3), Xueping Zhang^b, Tim Bell^c and Steve Cadigan^a

^aTechSolve, Inc., Cincinnati, USA

^bShanghai Jiao Tong University, Shanghai, PRC

^cMicroTek Finishing, Cincinnati, USA

Submitted by S. R. T. Kumara (1), Pennsylvania, USA

This paper presents investigations on high speed turning of Ti-6Al-4V alloy using super-finished cutting edge inserts generated by micro-machining process (MMP). In order to better understand the influence of super-finished cutting edges and their impact on active force components, tool face friction is analyzed. The tool-chip-work friction coefficients are obtained analytically using measured cutting forces under orthogonal cutting conditions and chip characteristics. The cutting forces and chip morphology are predicted accurately using a two dimensional finite element model (FEM) using ABAQUS. The turning tests conducted under flooded coolant conditions show that super-finished cutting edge inserts substantially enhance the tool life.

Keywords: Ti-6Al-4V, Super finished tool, tool face friction

1. Introduction

Titanium alloys such as Ti-6Al-4V have high specific strength, high toughness, high corrosion resistance, low density, bio-compatibility and are extensively used in aerospace, biomedical, chemical and many other industries. These alloys are difficult to machine due to their inherent properties such as low thermal conductivity, low modulus of elasticity and high chemical reactivity with other materials at elevated temperatures [1]. The machining of titanium (Ti-6Al-4V) alloy generates serrated and cyclic chips which are considered to be caused by adiabatic shearing [2-4]. Literature survey reveals that many experimental and numerical investigations have been made to study the cutting performance of this alloy with the aim of enhancing the machinability and productivity [3-8]. Some investigations have shown that machining performance of titanium alloys is increased by improving cutting tool material/geometry and coatings [5-6]. In this paper, the impact of super-finish prepared cutting edge of the uncoated tungsten carbide (WC/Co) inserts on machining performance is investigated for possible improvements in machining of Ti-6Al-4V alloy. Also, two dimensional (2-D) finite element model (FEM) is used to predict cutting forces precisely. In the past, most of the numerical investigations have been made using DEFORM software for two dimensional (2-D) orthogonal cutting of Ti-6Al-4V alloy [9-13]. DEFORM is based on the modified-Lagrangian rigid-plastic FEM, which cannot achieve the plastic deformation and therefore the residual stresses generated from

elastic recovery after unloading are not considered during the analysis [14]. During present investigations, ABAQUS has been used for numerical investigations that takes care of this aspect and overcomes DEFORM's inherent disadvantage [15-17].

To precisely predict cutting forces and chip morphology, it is important to determine the tool-chip-work friction coefficients. Shaw [18] proposed an approach of calculating tool-chip friction coefficient using sharp tool. However, cutting tools, in general, have a honed or chamfered cutting edge and it is reasonable to consider the tool-edge effect on cutting forces and tool temperatures [18]. This requires the determination of tool-chip-work friction coefficients. In most literatures, tool-chip-work friction coefficients have been determined empirically. Such as, an average value of friction coefficient of 0.7 to 0.9 have been recommended in DEFORM software [14]. Umbrello [9] in his analysis set tool-work friction coefficient as 0.7 while Ozel and Sima [10, 12] adopted tool-work friction coefficient of 0.85 for uncoated tool and 0.9 for coated tool. Several other investigators considered tool-chip friction coefficients as 0.3 [11, 17] and 0.5 [10, 15, 17] based on empirical formula [18]. It is obvious that the presumed or empirical determination of tool-chip-work friction coefficients cannot predict the machining performance accurately.

This paper proposes a new friction model to determine the friction coefficients of chip-tool-work based on Shaw's orthogonal cutting force model by incorporating 2-D experimental forces and chip morphology. The tool-chip-work friction coefficients are obtained analytically. A FEM is

established to simulate Ti-6Al-4V alloy high-speed dry cutting process using ABAQUS and it is validated by cutting forces and the chip morphology for different cutting parameters.

2. Super-finishing of cutting tools using Micro Machining Process (MMP)

The Micro Machining Process (MMP) is a unique method of super finishing. What makes this technology truly unique is its ability to selectively remove specific components of roughness while leaving others intact. The commercially available uncoated/coated inserts have certain amount of roughness and cutting edge characteristics which can be considered as a collection of "frequency ranges". The term "frequency" is used because at a micro level the peaks and valleys of the surface can be represented as a collection of different wavelengths of varying amplitudes. These frequencies can be characterized into four different ranges, with each successively higher range superimposed on the one below it.

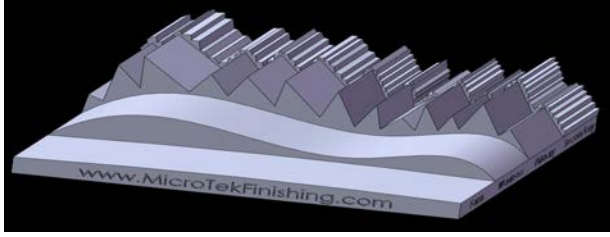


Fig. 1. Schematic of a cutting tool edge

The lowest frequency range is the expected "**Form**" of the cutting edge. Layered on top of the Form is the "**Waviness**" and layered on top of the Waviness is the "**Primary Micro Roughness**". Finally, layered on top of the Primary Micro Roughness is the "**Secondary Micro Roughness**", which results from the roughness on the surface of the cutting tool that was imparted on it during its manufacturing process and is transferred to the part being cut. Figure 2 shows cutting tool edge of a commercially available insert and super-finished cutting edge.

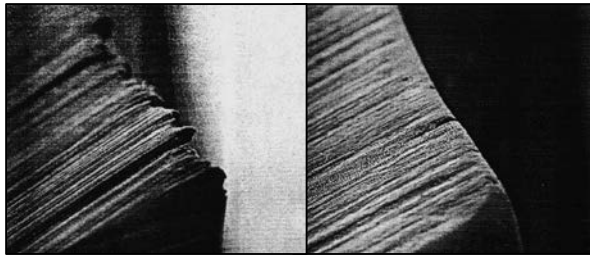


Fig. 2. Cutting Tool Edge (X500 Magnification)

3. Finite Element Model (FEM)

The FEM includes work material constitutive model, chip separation criterion, chip-tool-work friction condition, mesh and boundary conditions that are described below.

3.1 Material model of titanium alloy Ti-6Al-4V

In order to describe metal material behaviour subjected to a large strain, high strain rate and temperature-dependence visco-plasticity in dry cutting process, Ti-6Al-4V constitutive model adopts the following Johnson-Cook (J-C) model [19]

$$\bar{\sigma} = (A + B\bar{\epsilon}^n) \left[1 + C \ln\left(\frac{\dot{\bar{\epsilon}}}{\dot{\bar{\epsilon}}_0}\right) \right] \left[1 - \left(\frac{T - T_0}{T_{melt} - T_0} \right)^m \right] \quad (1)$$

Where $\bar{\sigma}$ is the equivalent stress; $\bar{\epsilon}$, the equivalent plastic strain; $\dot{\bar{\epsilon}}$, the plastic strain rate; $\dot{\bar{\epsilon}}_0$, the reference strain rate; T_{melt} , the melting temperature; T_0 is transition temperature defined as room temperature 25°C; A is the initial yield stress, B is the hardening modulus, C is the strain rate dependent coefficient, n is the work-hardening exponent, m is the thermal softening coefficient, A , B , C , n and m are material constants.

Johnson-Cook failure model [20] is employed to simulate the chip separation behaviour and the chip crack initiation or growth. Johnson-Cook failure model is based on the value of the equivalent plastic strain at element integration points. Damage parameter D is defined as

$$D = \sum \left(\frac{\Delta \bar{\epsilon}^{pl}}{\bar{\epsilon}_f^{pl}} \right) \quad (2)$$

Where $\Delta \bar{\epsilon}^{pl}$ is the increment of the equivalent plastic strain which is updated at every analysis increment; $\bar{\epsilon}_f^{pl}$ is the equivalent strain at failure and is expressed as:

$$\bar{\epsilon}_f^{pl} = \left[d_1 + d_2 \exp\left(d_3 \frac{p}{q}\right) \right] \left[1 + d_4 \ln\left(\frac{\dot{\bar{\epsilon}}^{pl}}{\dot{\bar{\epsilon}}_0}\right) \right] \left[1 + d_5 \left(\frac{T - T_0}{T_{melt} - T_0} \right) \right] \quad (3)$$

Where $\bar{\epsilon}_f^{pl}$ depends on the non-dimensional equivalent plastic strain rate of $\dot{\bar{\epsilon}}_0^{pl} / \dot{\bar{\epsilon}}_0$, the ratio of hydrostatic pressure to Mises equivalent stress p/q , temperature and the damage constants ($d_1 \sim d_5$). Failure is assumed to occur when the damage parameter D exceeds 1.

Johnson-Cook model and Johnson-Cook damage constants were obtained by Split Hopkinson Pressure Bar (SHPB) test performed under various strain rates and temperatures. The material parameters of Ti-6Al-4V have been reported in Table 1 [7, 8].

Table 1
Johnson-Cook model and its failure model's parameters of Ti-6Al-4V [7-8]

A (MPa)	B (MPa)	n	C	m
1200	1200	0.22	0.014	1.1

However, Johnson-Cook model experimentally measured by SHPB had certain limitation. The strain rates for the experiment of Ti-6Al-4V constitutive model reached 10^4 s^{-1} [8], which were far less than the strain rates during the actual metal cutting processes. The true strain rates reached $10^4 \sim 10^5 \text{ s}^{-1}$ [9], even higher. The Johnson-Cook constitutive model by SHPB is unable to describe the mechanical properties of high speed cutting. The determination of Johnson-Cook constitutive model is the key technique for the FEM simulation of machining operations. Modified Johnson-Cook constitutive model is shown in Table 2, which is validated by comparing FEM results with experimental measurement.

Table 2

Modified Johnson-Cook model of Ti-6Al-4V

A (MPa)	B (MPa)	n	C	m
1098	1092	0.93	0.014	1.1
d_1	d_2	d_3	d_4	d_5
-0.09	0.27	0.48	0.014	3.87

3.2 Material Properties of Workpiece and Tool Materials

Material Properties of Ti-6Al-4V and tool are shown in the following Table 3.

Table 3

The Properties of Ti-6Al-4V and Tool [4, 5]

Properties	Ti-6Al-4V	Tool
Expansion($\mu m \cdot m^{-1} \cdot ^\circ C^{-1}$)	$\partial(T) = 3.10^{-9} \cdot T + 7.10^{-6}$	4.9
Conductivity($W m^{-1} \cdot ^\circ C^{-1}$)	$\lambda(T) = 7.039e^{0.0011 \cdot T}$	59
Young's modulus (MPa)	$E(T) = 0.714T + 113375T$	650
Heat capacity($J / Kg \cdot ^\circ C$)	$C_v(T) = 505.64e^{0.0007 \cdot T}$	15
Density(g / cm^3)	4.43	14.5
Passion's ratio	0.34	0.25

3.3 Tool-chip interface friction model

Modified Coulomb friction model is adopted to capture the chip-tool and work-tool interface friction patterns, which contains two distinct regions: sticking region and sliding region. The normal stress magnitude acting on the contact point determines whether the contact area is in sticking or sliding state. The friction force of sliding region ($\mu\sigma < \tau_{max}$) is

$$\tau = \mu\sigma \quad (4)$$

The friction force of sticking region ($\mu\sigma \geq \tau_{max}$) is

$$\tau = \tau_{max} \quad (5)$$

Where μ is the coefficient of friction along the sliding zone,

τ_{max} is the material shear yield stress. The commonly accepted estimation of τ_{max} is expressed as

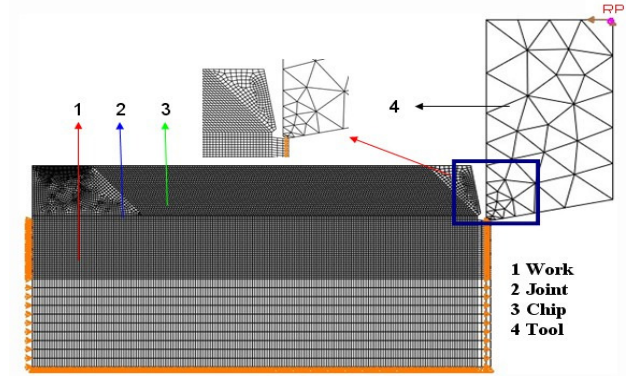
$$\tau_{max} = \sigma_y / \sqrt{3} \quad (6)$$

Where σ_y is the uniaxial yield flow stress of the work material.

However, σ_y is estimated by empirical value [21], which is assumed 500 MPa.

3.4 Mesh and boundary condition for orthogonal cutting FEM

The orthogonal (2-D) machining model for Ti-6Al-4V alloy geometrically consists of four parts [22]: (1) work, (2) the joint layer characteristic of a narrow band and material failure candidate element, (3) the chip layer, and (4) the cutting tool as shown in Figure 3. The bottom surface of work is restrained in the feed direction, the left and right ends are restrained in the cutting direction. The tool is regarded as a rigid body moving left along the cutting direction.

**Fig.3.** FEM of 2D orthogonal dry cutting Ti-6Al-4V

3.5 Determination of tool-chip-work friction coefficients by measured cutting forces

All the tests have been conducted using a Hardinge Cobra CNC Turning Center which is interfaced with the PC and a three-dimensional (3-D) Kistler Dynamometer for on-line force data acquisition. The experimental set-up is shown in Fig. 4.

**Fig.4.** Experimental set-up of Ti-6Al-4V turning test

The conditions of the orthogonal turning tests are provided in the following Table 4.

Table 4

Machining parameters for Ti-6Al-4V orthogonal turning test

Work Material	Tube, 50.8mm in diameter and 3.175 mm wall thickness
Tool Holder	Type CTGPL 164
Cutting Tool	Uncoated Carbide: (Grade K313)
(Insert TPG 432)	Coated Carbide: (Grade KC5010)
	Super-finished Edge: (Grade K313)
Rake Angles	0° and 5°
Relief Angle	11° and 6°
Cutting Speeds	100 m/min
Feed Rates	0.076 mm/rev, 0.1016 mm/rev and 0.127mm/rev
Cut Length/Test	1.016 mm
Cutting Fluid	No coolant (Dry)

During the orthogonal (2-D) turning tests, the measured forces include (i) cutting force and (ii) thrust force, whose direction and numerical values are shown in Figure 5 and Table 5, respectively.

Table 6
Tool-Chip-Work friction coefficients

Variable	tool-chip friction coefficient		tool-work friction coefficient	
	Rake angle 0°	Rake angle 5°	Rake angle 0°	Rake angle 5°
Feed rate (mm/rev)				
0.076	0.249	0.325	1.083	0.986
0.1016	0.213	0.287	1.115	1.111
0.127	0.176	0.249	1.172	1.184

The chip morphology of Ti-6Al-4V is observed to be saw-tooth as shown in Figure 7. h_{max} is the distance between chip peak and the bottom, h_{min} is that between chip valley and peak. The distance between C1 and C2 is the chip-pitch, and the average value of which is P_c . The mean distance between C1 and D1 is P. Therefore, the cutting ratio γ is expressed by the distance P_c and P:

$$\gamma = \frac{P_c}{P} \quad (15)$$

The measured cutting ratio γ is approximately 0.84 when the rake angle is 0° and the feed rate is 0.127mm/rev. By combining the formulas (16) and (17), shear angle obtained is approximately 40° and the friction angle of tool-chip interface is 10°.

$$\phi = \tan^{-1} \left(\frac{r \cos \alpha}{1 - r \sin \alpha} \right) \quad (16)$$

$$\phi = \frac{\pi}{4} - \frac{1}{2}(\beta - \alpha) \quad (17)$$

The tool-chip-work friction coefficients are calculated by combining the equations (7) to (14). Through the same method, tool-chip-work friction coefficients for other cutting condition are calculated in Table 6.

For the same rake angle, the shear angle and tool-work friction coefficients increase with the increase in feed rate, otherwise are tool-chip friction coefficients. However, the tool-work friction coefficients are 3.03–6.66 times larger than that of tool-chip friction coefficients. For the same feed-rate, the tool-chip friction coefficients increase with the increase in rake angle. The normal stresses decrease with increase in rake angle and the ratio of material yield strength to normal stress increases.

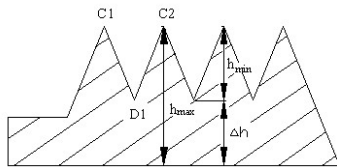


Fig.7. Schematic diagram of saw-tooth morphology

4. FEM Validation

4.1 Predicted force and validation

The measured and predicted cutting forces using FEM analysis are compared in Tables 7 and 8 for the cutting speed of 100 m/min and two (0°, 5°) rake angles.

Table 7
Force validation when rake angle 0°

Feed Rates (mm/rev)	Measured Value	Simulated value	Error (%)
Cutting force (N)			
0.076	501.626	521.893	4.04
0.1016	634.672	651.061	2.58
0.127	736.091	748.719	1.72
Thrust force (N)			
0.076	254.527	256.973	0.96
0.1016	307.505	302.056	1.77
0.127	302.79	282.573	6.68
Resultant force (N)			
0.076	562.506	581.728	3.42
0.1016	705.243	717.7174	1.77
0.127	795.935	800.2672	0.54

Table 8
Force validation when rake angle 5°

Feed Rates (mm/rev)	Measured Value	Simulated value	Error (%)
Cutting force (N)			
0.076	477.072	502.709	5.37
0.1016	613.587	636.541	3.74
0.127	725.327	742.162	2.32
Thrust force (N)			
0.076	245.586	237.803	3.17
0.1016	276.190	262.026	5.13
0.127	288.556	274.366	4.92
Resultant force (N)			
0.076	536.573	556.117	3.64
0.1016	672.882	688.362	2.30
0.127	780.618	791.253	1.36

The results show that experimental cutting forces have close agreement with the predicted cutting forces (error ~ 5.37%). The error of thrust forces predicted is less than 7%, which can be further improved with the accuracy of measured shear angle. The prediction error of resultant force is ~ 3.64%. The agreements between the predicted and measured forces validate the FEM for orthogonal (2-D) dry cutting of Ti-6Al-4V alloy accurately regardless of machining conditions.

4.2 Predicted chip morphology and validation

The predicted and measured saw-tooth chip adopting feed rate of 0.127 mm/rev, rake angle of 0°, and the cutting speed of 100m/min are shown in Figure 8. The average distance of the chip pitch is 0.1219 mm, and distance between chip peak to valley is 0.1096 mm. The corresponding predicted values are 0.1156 mm and 0.110 mm, respectively. The prediction errors are 5.2% and 0.4% respectively. These results verify the FEM in terms of chip morphology.

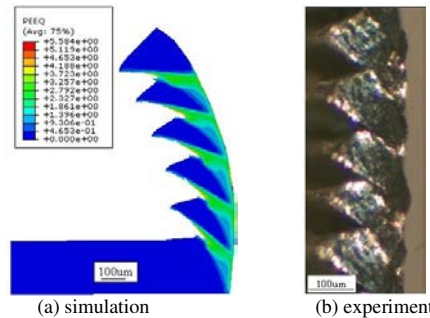


Fig.8. Simulated chip morphology compared with experiment

An oblique turning test was conducted to see the effect of super-finishing the cutting edge on tool-life. Before conducting the test, the average surface roughness values (R_a) of uncoated (K313 Grade), coated (KC5010 Grade) and super-finished cutting edge (K313 Grade) were measured which were 0.097, 0.314 and 0.084 μm , respectively, at a cut-off length of 1.25 mm. The results for tool wear are shown in Fig. 9. The results clearly show that tool-life substantially increases when super-finished cutting edge inserts are used. It seems that super-finishing the cutting edge provides better contact and distribution of cutting pressure and distribution of heat at work-tool-chip contact zone, thus, enhancing the tool-life.

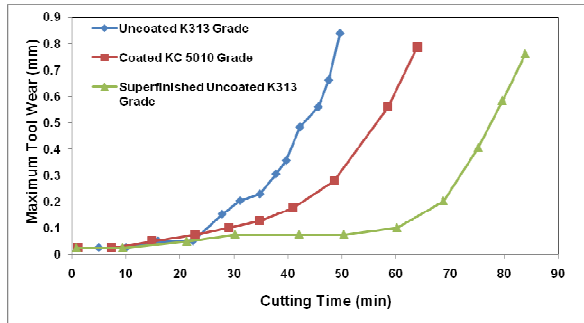


Fig.9. Maximum tool wear v/s machining time using uncoated, coated, and super-finished cutting edge tool (cutting speed: 100 m/min, feed-rate: 0.075 mm/rev, depth of cut: 1.00 mm, coolant: (5% vol.) Trim Sol)

This confirms that super-finishing the cutting edge of the inserts using MMP have a positive impact on the tool life and reliability of cutting tools when applied correctly.

5. Conclusions

Tool-chip-work friction coefficients are obtained analytically using orthogonal (2-D) cutting experimental forces and chip characteristics. A FE model for high speed dry machining of Ti-6Al-4V alloy is established using ABAQUS, which is validated in terms of predicted forces and the chip morphology. The specific conclusions include:

- 1) The tool-work friction coefficients are 3.03 to 6.66 times larger than that of tool-chip friction coefficients. The tool-chip friction coefficients decrease with feed-rates, and otherwise are the tool-work friction coefficients.
- 2) The predicted cutting forces, thrust forces and resultant forces by the FE model agree well with the experimentally measured forces. The prediction errors are less than 6%, 7% and 4% respectively. The errors are lower than 5.2% and 0.4%, respectively in terms of the predicted average value of chip pitch and between the chip valley and peak.
- 3) Super-finishing the cutting edge of the inserts using MMP substantially enhances the tool life during the high speed machining of Ti-6Al-4V titanium alloy.

Acknowledgement

The authors gratefully acknowledge the support by the National Science Foundation (NSF) award number CMMI - 0757954.

References

- [1] Byrne, G., Dornfeld, D. and Denkena, B., 2003, Advanced Cutting Technology, CIRP Annals 52(2):483–507.
- [2] Cotterell, M. and Byrne, G., 2008, Dynamics of Chip Formation during Orthogonal Cutting of Titanium Alloy Ti-6Al-4V, CIRP Annals 57:93–96.
- [3] Komanduri, R. and von Turkovich, B. F., 1981, New Observations on the Mechanism of Chip Formation When Machining Titanium Alloys, Wear 69:179–188.
- [4] Shivpuri, R., Hua, J., Mittal, P. and Srivastava, A. K., 2002, Microstructure-Mechanics Interactions in Modelling Chip Segmentation During Titanium Machining, CIRP Annals 51(1):71–74.
- [5] Corduan, N., et al. 2003, Wear Mechanisms of New Tool Materials for Ti-6Al-4V High Performance Machining, CIRP Annals 52(1):73–76.
- [6] Bouzakis, K-D., et al. 2009, Application in Milling of Coated Tools with Rounded Cutting Edges after Film Deposition, CIRP Annals 58(1):61–64.
- [7] Nemat-Nasser, S., et al. 2001, Dynamic Response of Conventional and Hot Isostatically Pressed Ti-6Al-4V Alloys: Experiments and Modelling, Mechanics of Materials 33:425–439.
- [8] Lee, W. S. and Lin, C. F., 1998, Plastic Deformation and Fracture Behaviour of Ti6Al4V Alloy Loaded with High Strain Rate Under Various Temperatures, Materials Science and Engineering, 241:48–59.
- [9] Umbrello, D., 2008, Finite Element Simulation of Conventional and High Speed Machining of Ti-6Al-4V Alloy, Journal of Materials Processing Technology, 196: 79–87.
- [10] Sima, M. and Ozel, T., 2010, Modified Material Constitutive Models for Serrated Chip Formation Simulations and Experimental Validation in Machining of Titanium Alloy Ti-6Al-4V, International Journal of Machine Tools & Manufacture, 50: 943-960.
- [11] Shao, F. and Zhang, Q., 2010, Finite Element Simulation of Machining of Ti-6Al-4V Alloy with Thermo-dynamical Constitutive Equation, The International Journal of Advanced Manufacturing Technology, 49: 431–439.
- [12] Ozel, T., Sima, M., Srivastava, A. K. and Kaftanoglu, B., 2010, Investigations on the Effects of Multi-Layered Coated Inserts in Machining Ti-6Al-4V Alloy with Experiments and Finite Element Simulations, CIRP - Manufacture Technology, 59: 77-82.
- [13] Zhao, W. and He, N., 2009, Effect Mechanism of Nitrogen Gas on Chip Formation in High Speed Cutting of Ti-6Al-4V Based on FEM Simulation, Material Science Forum, 626-627: 177-182.
- [14] Jeffrey, F., 2003, DEFORM -2D Version 8.1 User's Manual, Science Forming Technologies Corporation.
- [15] Chen, L., El-Wardany, T. L., 2004, Modeling the Effects of Flank Wear and Chip Formation On Residual Stress, CIRP Annals - Manufacturing Technology, 53: 95-98.
- [16] Yang, X. and Liu, C. R., 2002, A New Stress-Based Model of Friction Behaviour in Machining and Its Significant Impact on Residual Stresses Computed by Finite Element Method, International Journal of Mechanical Science, 44: 703-723.
- [17] Anurag, S. and Guo, Y. B., 2010, A New Finite Element Approach Without Chip Formation to Predict Residual Stress Profile Patterns in Metal Cutting, International Manufacturing Science and Engineering Conference, 38: 33-40.
- [18] Shaw, M. C., 1984, Metal Cutting Principles, Clarendon Press.
- [19] Johnson, G. R. and Cook, W. H., 1983, A Constitutive Model and Data for Metals Subjected to Large Strains, Strain Rates and High Temperatures, Proceedings of the Seventh International Symposium on Ballistics.
- [20] Johnson, G. R. and Cook, W. H., 1985, Fracture Characteristics of Three Metals Subjected to Various Strains, Strain Rates, Temperatures and Pressures, Engineering Fracture Mechanics, 21: 31-48.
- [21] Karlson, H., 2003, ABAQUS Analysis User's Manual Version 6.4, HSK, Inc, U.S.A.
- [22] Wang, H. and Zhang, X., 2009, FEM Modelling on Hard Cutting Bearing Steel and Machined Surface Residual Stress Analysis, SJTU, Shanghai, China.
- [23] Srivastava, A. K. and Iverson, J., 2010, An Experimental Investigation into the High Speed Turning of Ti-6Al-4V Titanium Alloy, International Manufacturing Science and Engineering Conference, Erie, PA, USA.